University of Bristol - Explore Bristol Research
General rights

The Hippocampal Engram Maps Experience But Not Place

Kazumasa Z. Tanaka[1],*, Hongshen He[1,2], Anupratap Tomar[1], Kazue Niisato[1], Arthur J.Y. Huang[1], Thomas J. McHugh[1,2]*

5   [1]Laboratory for Circuit and Behavioral Physiology, RIKEN Brain Science Institute, 2-1 Hirosawa, Wakoshi, Saitama, Japan

[2]Department of Life Sciences, Graduate School of Arts and Sciences, University of Tokyo, Tokyo, Japan

*Corresponding author. Email: kazumasa.tanaka@riken.jp (K.Z.T), tjmchugh@brain.riken.jp
10   (T.J.M)

15

20

25

30

Episodic memories are encoded by a sparse population of hippocampal neurons. In mice optogenetic manipulation of this memory engram established that these neurons are indispensable and inducing for memory recall. However, nothing is known about their *in vivo* activity or precise role in memory. We found that during memory encoding only a fraction of CA1 place cells are engram neurons, distinguished by firing repetitive bursts paced at the theta frequency. During memory recall these neurons remained highly context specific, yet demonstrated preferential remapping of their place fields. These data demonstrate a dissociation of precise spatial coding and contextual indexing by distinct hippocampal ensembles and suggest the hippocampal engram serves as an index of memory content.

One Sentence Summary: Hippocampal engram neurons are context specific, yet spatially unreliable, suggesting they map an internal representation of memory.

Numerous theories have attempted to link the physiology of the hippocampus with its role in episodic memory (*1, 2*), however experimental tests of these ideas remain scarce. One prevailing model suggests the hippocampal memory trace contains rich information about the animal's current location within the cognitive domain, providing a spatial framework on which events and items can be anchored and related (Cognitive Map Theory (*3, 4*)). This is supported by data demonstrating synaptic plasticity stabilizes these hippocampal maps and that animals can reliably recall these representations, even at remote time points (*5, 6*). An alternate, although not mutually exclusive, hypothesis, the Memory Index Theory, asserts that the hippocampal memory trace is primarily an index that provides rapid and efficient access to the content of an episodic memory stored in the neocortex (*7, 8*). This theory is agnostic to the information content in the hippocampus, emphasizing its role reactivating downstream cortical cells, with plasticity serving to establish a link between the hippocampal index and the neocortical activity pattern.

Although place cell physiology supports the Cognitive Map Theory (*9*), behavioral studies using contextual fear conditioning (CFC (*10*)) may be better interpreted via the Memory Index Theory.

In CFC the contextual representation is index-like because its formation requires conjunctive exposure to cues and its rapid recall does not require physical exploration of the environment (*11*). Moreover, the expression of activity-induced genes, such as c-Fos, is rapidly and robustly induced in a unique neuronal ensemble following presentation of novel stimuli configurations

5   and is thought to define the neuronal substrates of the contextual representation (*12*, *13*). Recent studies (*14*) further strengthen this view, demonstrating that inhibition of hippocampal engrams can block memory recall in contextual tasks, while activation can drive context-triggered behavior (*15*, *16*). The link between this contextual memory representation and precise locations or routes represented by place cells during exploration remains unknown.

10   We therefore conducted tetrode recordings from CA1 pyramidal cells in freely moving c-Fos-tTA transgenic mice infused with AAV-TRE-ChR2-EYFP virus. Doxycycline was removed from the diet of the mice, triggering labeling of c-Fos expressing (positive) cells with ChR2, and place cell activity was recorded as mice explored a novel context (A; encoding context; Fig. 1A). The next day (12-14 hours later; Fig. S1) the animals were re-exposed to context A (recall) to

15   examine the stability of the spatial map. CA1 was stimulated with pulses of blue light (10 mW, 0.5 Hz, 15 ms) to identify the subset of cells which expressed ChR2 as a result of c-Fos expression during the first session (Fig. 1B and fig. S2). In a separate cohort of mice we verified this OptID protocol did not impact excitability or spatial coding properties of the labeled neurons (Fig. S3). Across the 7 animals used in this study $19.59 \pm 2.65\%$ of putative pyramidal cells

20   exhibited light-induced spikes, and thus identified as c-Fos positive (Fig. 1C). This fraction is consistent with previous reports (*17*). Finally, the same mice explored a distinct environment (B) to examine context specific activity (*18*).

We first examined the spatial firing of c-Fos positive neurons as the animals explored the novel context A. The majority of these cells had place fields in the labeled context (Fig. 1D; 79.31%, see Methods for place field criteria). However, a large fraction of the active place cells were not labeled with ChR2 (Fig. 1E; 75.53%). Although physiologically similar, with indistinguishable peak firing rates (Fig. 1F, pos: 6.99 ± 1.06 Hz; neg: 6.06 ± 0.53 Hz, $W = 640$, $p = 0.20$), c-Fos positive place cells exhibited significantly higher mean firing rates (Fig. 1G, pos: 1.43 ± 0.22 Hz; neg 0.77 ± 0.11 Hz, $W = 357$, $p = 5.4e\text{-}05$). Accordingly, positive cells had larger place fields (Fig. 1H, pos: 28.00 ± 3.50 cm^2; neg: 17.97 ± 1.79 cm^2, $W = 517$, $p = 0.0085$) and on average, their spikes carried lower spatial information (Fig. 1I, pos: 0.69 ± 0.81 bits/spk; neg: 1.21 ± 0.83 bits/spk, $W = 1191$, $p = 0.001$).

We next analyzed the temporal structures of spike activity during exploration (A, encoding). Inter-spike-interval (ISI) analysis revealed that spikes from engram cells were more likely to occur in burst (3-15 ms ISI) (Fig. 2A). These neurons had significantly higher burst rates (Fig. 2B, pos: 16.80 ± 3.04 bursts/min; neg: 8.87 ± 1.44 bursts/min, $W = 1243$, $p = 0.00018$) and shorter average inter-burst-intervals (IBI) (Fig. 2C, IBI: pos: 6.55 ± 1.30 sec; neg: 16.27 ± 2.15 sec, $W = 415$, $p = 0.00042$). Burst events in c-Fos positive neurons were preferentially spaced at ~125 mSec, an interval corresponding to the 8 Hz theta rhythm in the hippocampus. Bursts from these neurons were significantly more theta modulated than bursts from c-Fos negative cells (Fig. 2, D to F; theta modulation index, $W = 418$, $p = 0.0009$; theta power in burst spectrum, $W = 1151$, $p = 4.8e\text{-}05$). We thus defined theta-burst events (TBE) as bursts repeated at IBIs of 83-167 msec (6-12 Hz) and compared this property across the groups. During exploration of the novel context A, c-Fos positive cells showed higher rates of TBEs than negative place cells (Fig,. 2, G and H, pos: 5.44 ± 1.41 bursts/min; neg: 2.58 ± 0.53 bursts/min, $W = 417.5$, $p = 0.00046$)

and longer repetitions of bursts (Fig2, I and J, pos: 2.68 ± 0.095 bursts/event; neg: 2.56 ± 0.052

bursts/event, W = 652.5, p = 0.20; 2I, max TBE length: pos: 7.13 ± 0.78 bursts; neg: 5.28 ± 0.34

bursts, W = 542, p = 0.022). These burst features were no longer prominent in ChR2-labeled

neurons when the animals explored context B (Fig. S5), suggesting their involvement in

5   contextual encoding.

We then examined the temporal modulation of place cell spiking by the oscillatory population

activity in the LFP (A, encoding). CA1 neurons can be entrained by the theta (6-12 Hz) rhythm,

as well as by slow (30-50 Hz) and fast (55-85 Hz) gamma oscillations, which correlate with CA3

and entorhinal cortical inputs to CA1 respectively (*19*). Spikes from c-Fos positive and negative

10   cells were similarly theta entrained and preferred the ascending phase of the oscillation (Fig. 3, A

and B; mean preferred phase, pos: 229.9 ± 1.73°; neg: 199.2 ± 1.85°, W = 0.42, p = 0.81).

However, TBE spikes in positive neurons preferentially occurred during the descending phase,

while those in negative neurons remained locked to the ascending phase (Fig. 3, C to E; mean

preferred phase: pos: 170.7 ± 1.86°; neg: 325.7 ± 1.54°, W = 62.66, p = 2.5e-14). Next, to

15   address any differences in coupling of positive and negative neurons to CA1 inputs, we

examined spikes during gamma events. Significantly more spikes from positive neurons occurred

during fast gamma events and a larger fraction of these neurons were phase locked to fast gamma

compared to the c-Fos negative population (Fig. 3F; percent spikes: pos: 2.62 ± 0.17%; neg: 2.19

± 0.11%, W = 1067, p = 0.0072; percent cells phase-locked: pos: 26.09%; neg: 14.08%, chi-

20   squared test, p = 0.0014). There was no significant difference in spiking or phase locking

between the groups during slow gamma (Fig. 3G; percent spikes: pos: 5.81 ± 0.31%; neg: 5.53 ±

0.23%, W = 888, p = 0.53; percent cells phase-locked: pos: 26.09%; neg: 29.58%, chi-squared

test, p = 0.62). These data suggest that while both populations of neurons are similarly tuned to

CA3-driven excitation, c-Fos positive neurons may be more responsive to input from the entorhinal cortex, resulting in the temporal shift in their unique theta-paced bursting.

Finally, we examined hippocampal activity during memory recall and assessed the stability of the spatial representation of engram cells when animals re-visited the labeling context (A). Contrary to expectations of a spatial memory trace, many of these cells shifted their firing locations during the second visit (Fig. 4A). In positive neurons the average correlation of the firing rate maps from the encoding and recall sessions was close to zero, significantly lower than that from negative place cells (Fig. 4B and fig. S6; pos: 0.079 ± 0.070; neg: 0.31 ± 0.052, W = 560, p = 0.010). However, correlations of the mean firing rate, independent of position, were similar across both populations of cells (Fig. 4C; pos: 0.36 ± 0.053; neg: 0.36 ± 0.029, W = 412, p = 0.81), suggesting c-Fos positive neurons represent contextual information in a different manner. Therefore, we examined their activity in a distinct context. When animals explored context B, many c-Fos positive cells remained silent (Fig. 4A and fig. S6; 43.5% of pos place cells had peak rate < 1Hz; peak firing rate context A: 6.99 ± 1.06 Hz; context B: 3.42 ± 0.76 Hz, W = 392, p = 0.005). Consequently, there were fewer c-Fos positive place cells and the spatial information of these neurons was smaller than in context A (Fig. 4, D and E, chi-squared = 6, p = 0.014; 4E, two-way ANOVA, significant interaction, $F_{(1,89)} = 4.9$, p = 0.029; spatial info: context A: 0.89 ± 0.21 bit/sec; context B: 0.32 ± 0.071 bit/sec, W = 396, p = 0.0066). In contrast, the average spatial information carried by c-Fos negative place cells was unchanged (Fig. 4F,: context A: 0.51 ± 0.064; B: 0.37 ± 0.044 bit/sec, W = 2643, p = 0.30), although these cells typically shifted the location of their spatial firing ('remapped') in the new context (Fig4G; pos: 0.31 ± 0.052; neg: 0.013 ± 0.052, W = 982, p = 0.00029). These data are consistent with the hypothesis that engram cells do not necessarily represent reliable spatial information about the

external world, but rather through their net activity serve as an index to episodic information stored elsewhere in the brain (*7,8*). We therefore sought to discriminate contexts only from firing rate correlations of a subpopulation of neurons. We randomly sub-sampled c-Fos positive neurons and an equivalent number of c-Fos negative place cells and calculated the correlation of the mean firing rates of each population between context A (encoding) and A (recall) or between context A (encoding) and B (novel), repeating the procedure 1,000 times (see methods). As a population, the firing rate of c-Fos positive place cells reliably discriminated the two contexts, while the firing rate of the ensemble of negative cells did not (Fig. 4H; probability to find a higher correlation in A/B than A/A, p = 0.002 for pos ensemble, p = 0.57 for neg ensemble). This was also evident in the discrimination index (Fig. 4I; probability to find a greater index in neg than pos ensemble, p = 0.049). In contrast to the negative ensemble, context discrimination from firing rate correlations of c-Fos positive cells was prominent early in the recall session, demonstrating high correlation to the average rate of the encoding session during the first few minutes, or even the first 10 seconds (Fig. 4J and fig. S7; probability to find a higher correlation in neg than pos ensemble, p = 0.055, 0.038, 0.011, 0.230, 0.906, 0.754 for 1-6 min bins, p = 0.046 for the first 10 sec bin), suggesting the rapid reactivation of contextual representation by the subset of engram neurons. These data demonstrate that engram cells are place cells with lower spatial stability and accuracy, but with activity that can reliably and quickly reflect contextual identity.

When animals explore a novel context an engram is formed by a fraction of the place cells, suggesting that the plasticity involved in engram formation is distinct from that for formation of place fields. During encoding in the labeled context, engram neurons demonstrate repetitive theta frequency bursts. *In vitro* this pattern of action potentials is known to produce a form of long-

term potentiation mediated by BDNF secretion and dependent on c-Fos expression (*20*, *21*). c-Fos expression and theta bursts have been observed in CA1 when animals perform a non-spatial memory task (*22*, *23*), suggesting this activity may be a signature of hippocampal engrams indexing broader types of memories.

Our study does not support the idea that the hippocampal engram simply encodes spatial memory because these neurons do not maintain their firing locations in the same environment across time. Instead, we propose that these cells may serve as an index for contextual memory through a shift of firing rates. Compared to other place cells, during recall these c-Fos positive neurons rapidly spike at rates highly correlated to their activity during the encoding period and are preferentially silent in a distinct context. This may explain why optogenetic stimulation of the hippocampal engram can influence contextual memory recall (*24*) (Fig. S8), despite lacking temporally meaningful pattern of spikes. Inhibition of the CA1 engram reduces downstream cortical reactivation (*25*), consistent with a role in indexing. Our data suggest that unique ensembles of hippocampal neurons simultaneously support distinct domains of episodic memories – spatially reliable c-Fos negative neurons for configurational coding and spatially unstable engrams for contextual indexing.

References and Notes:

1. M. L. Shapiro, H. Eichenbaum, Hippocampus as a memory map: synaptic plasticity and memory encoding by hippocampal neurons. *Hippocampus*. **9**, 365–384 (1999).

2. G. Buzsáki, E. I. Moser, Memory, navigation and theta rhythm in the hippocampal-entorhinal system. **16**, 130–138 (2013).

3. J. O'Keefe, L. Nadel, *The hippocampus as a cognitive map* (Oxford University Press, USA, 1978).

4. O. Jensen, J. E. Lisman, Position reconstruction from an ensemble of hippocampal place cells: contribution of theta phase coding. *J Neurophysiol*. **83**, 2602–2609 (2000).

5. C. Kentros *et al.*, Abolition of long-term stability of new hippocampal place cell maps by

NMDA receptor blockade. *Science*. **280**, 2121–2126 (1998).

6.   T. J. McHugh, K. I. Blum, J. Z. Tsien, S. Tonegawa, M. A. Wilson, Impaired hippocampal representation of space in CA1-specific NMDAR1 knockout mice. *Cell*. **87**, 1339–1349 (1996).

7.   T. J. Teyler, P. DiScenna, The hippocampal memory indexing theory. *Behav Neurosci*. **100**, 147–154 (1986).

8.   T. J. Teyler, J. W. Rudy, The hippocampal indexing theory and episodic memory: updating the index. *Hippocampus*. **17**, 1158–1169 (2007).

9.   R. M. Grieves, K. J. Jeffery, The representation of space in the brain. *Behav. Processes*. **135**, 113–131 (2017).

10.   J. J. Kim, M. S. Fanselow, Modality-specific retrograde amnesia of fear. *Science*. **256**, 675–677 (1992).

11.   J. W. Rudy, R. C. O'Reilly, Conjunctive representations, the hippocampus, and contextual fear conditioning. *Cogn Affect Behav Neurosci*. **1**, 66–82 (2001).

12.   J. F. Guzowski, B. L. McNaughton, C. A. Barnes, P. F. Worley, Environment-specific expression of the immediate-early gene Arc in hippocampal neuronal ensembles. **2**, 1120–1124 (1999).

13.   M. VanElzakker, R. D. Fevurly, T. Breindel, R. L. Spencer, Environmental novelty is associated with a selective increase in Fos expression in the output elements of the hippocampal formation and the perirhinal cortex. **15**, 899–908 (2008).

14.   L. G. Reijmers, B. L. Perkins, N. Matsuo, M. Mayford, Localization of a stable neural correlate of associative memory. *Science*. **317**, 1230–1233 (2007).

15.   S. Tonegawa, X. Liu, S. Ramirez, R. Redondo, Memory Engram Cells Have Come of Age. *Neuron*. **87**, 918–931 (2015).

16.   S. A. Josselyn, S. Köhler, P. W. Frankland, Finding the engram. **16**, 521–534 (2015).

17.   K. K. Tayler, K. Z. Tanaka, L. G. Reijmers, B. J. Wiltgen, Reactivation of neural ensembles during the retrieval of recent and remote memory. *Current Biology* (2013).

18.   Local field potential (LFP) and single unit spiking were recorded during every session, as well as during pre-/post-exposure rest to ensure recording stability (Fig S4).

19.   L.L. Colgin, T. Denninger, M. Fyhn, T. Hafting, T. Bonnevie, O. Jensen, M.B. Moser, E.I. Moser, Frequency of gamma oscillations routes flow of information in the hippocampus. *Nature*. **462**, 353–357 (2009).

20.   E. Edelmann *et al.*, Theta Burst Firing Recruits BDNF Release and Signaling in

Postsynaptic CA1 Neurons in Spike-Timing-Dependent LTP. *Neuron*. **86**, 1041–1054 (2015).

21.   B. Kuzniewska *et al.*, Brain-derived neurotrophic factor induces matrix metalloproteinase 9 expression in neurons via the serum response factor/c-Fos pathway. *Mol. Cell. Biol.* **33**, 2149–2162 (2013).

22.   E. Amin, J. M. Pearce, M. W. Brown, J. P. Aggleton, Novel temporal configurations of stimuli produce discrete changes in immediate-early gene expression in the rat hippocampus. *European Journal of Neuroscience*. **24**, 2611–2621 (2006).

23.   T. Otto, H. Eichenbaum, S. I. Wiener, C. G. Wible, Learning-related patterns of CA1 spike trains parallel stimulation parameters optimal for inducing hippocampal long-term potentiation. *Hippocampus*. **1**, 181–192 (1991).

24.   T. J. Ryan, D. S. Roy, M. Pignatelli, A. Arons, S. Tonegawa, Memory. Engram cells retain memory under retrograde amnesia. *Science*. **348**, 1007–1013 (2015).

25.   K. Z. Tanaka *et al.*, Cortical Representations Are Reinstated by the Hippocampus during Memory Retrieval. *Neuron*. **84**, 347–354 (2014).

26.   L. M. Y. Yu, D. Polygalov, M. E. Wintzer, M.-C. Chiang, T. J. McHugh, CA3 Synaptic Silencing Attenuates Kainic Acid-Induced Seizures and Hippocampal Network Oscillations. *eNeuro*. **3**, ENEURO.0003–16.2016 (2016).

27.   R. Boehringer *et al.*, Chronic Loss of CA2 Transmission Leads to Hippocampal Hyperexcitability. *Neuron*. **94**, 642–655.e9 (2017).

28.   E. A. Mankin *et al.*, Neuronal code for extended time in the hippocampus. *PNAS*. **109**, 19462–19467 (2012).

29.   W. E. Skaggs, B. L. McNaughton, K. M. Gothard, E. J. Markus, An information-theoretic approach to deciphering the hippocampal code. *Proceedings of Advances in Neural Processing Systems*. **5**, 1030–1037.

30.   J. K. Leutgeb, S. Leutgeb, M.-B. Moser, E. I. Moser, Pattern separation in the dentate gyrus and CA3 of the hippocampus. *Science*. **315**, 961–966 (2007).

31.   C. Koch, I. Segev, *Methods in Neuronal Modeling* (MIT Press, 1998).

32.   K. Mizuseki, K. Diba, E. Pastalkova, G. Buzsáki, Hippocampal CA1 pyramidal cells form functionally distinct sublayers. *Nat. Neurosci.* **14**, 1174–1181 (2011).

33.   S. J. Middleton, T. J. McHugh, Silencing CA3 disrupts temporal coding in the CA1 ensemble. *Nat. Neurosci.* **19**, 945–951 (2016).
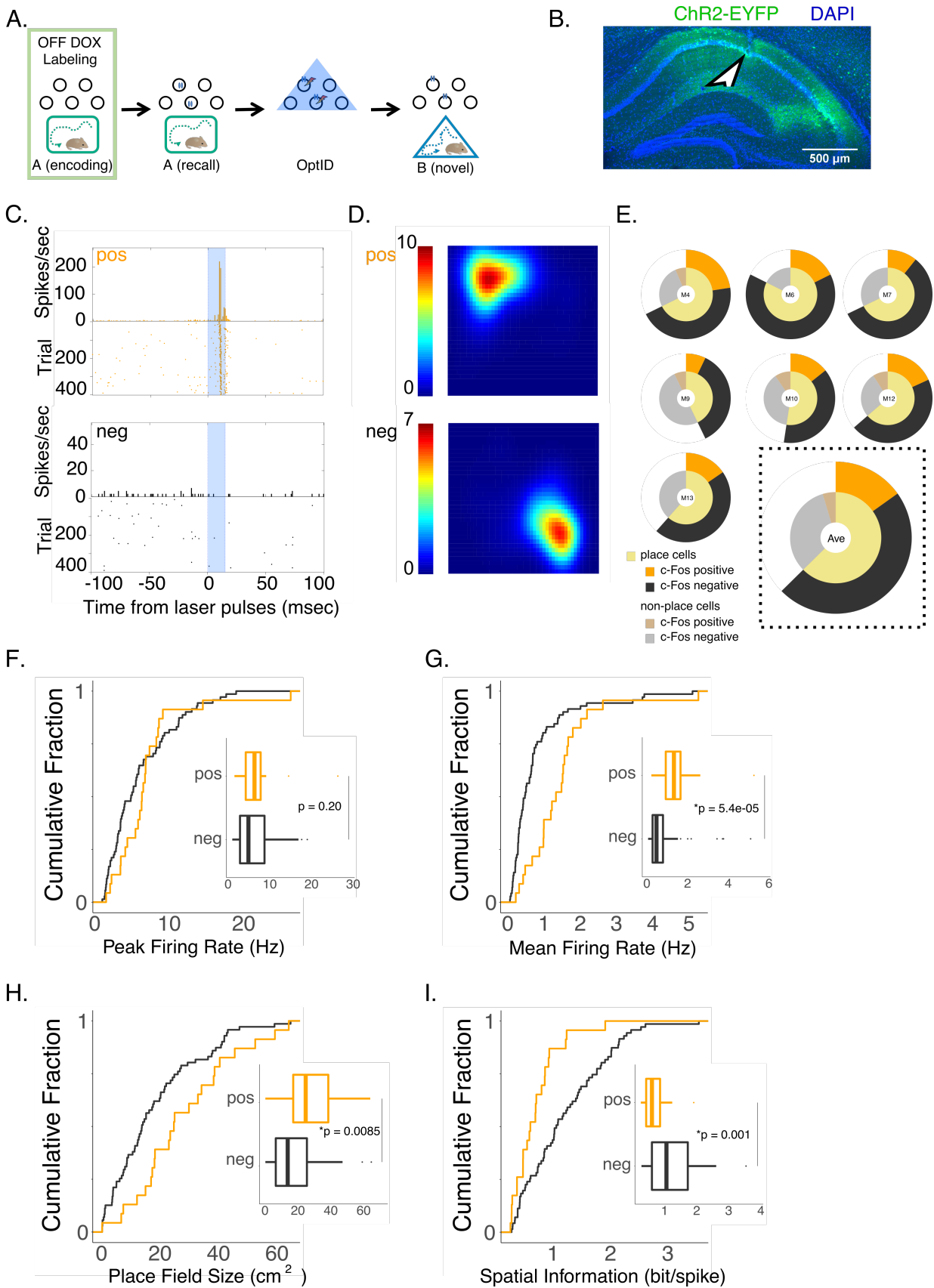
Acknowledgments

Supplementary Materials:

Materials and Methods

Figures S1-S8

References (*26-33*)

5

Fig. 1. c-Fos induction in a fraction of place cells during exploration of a novel context. **A.** A schematic of the experimental protocol. Mice were exposed to a novel context (A, encoding) during OFF DOX, followed by re-exposure to the same context (A, recall). Twenty-four hours after A (encoding), labeled cells were identified through light-induced spikes. Finally, mice explored a distinct context B (novel). See Materials and Methods for the detailed procedure. **B.** A representative image of a coronal section showing ChR2-EYFP (green) expression in the dorsal CA1 of the hippocampus. A white arrowhead indicates a tetrode location. **C.** Peri-stimulus time histogram of representative single units classified either c-Fos labeled (pos) or not labeled (neg). Blue areas represent light on epochs (15 msec). **D.** Firing rate maps of representative place cells showing location-specific firing during exploration in context A (encoding). **E.** Pie plots describing percentages of each cell types in recorded animals (N = 7), and their average in the dashed square. **F – I.** Cumulative density plots with inset boxplots comparing peak firing rates (F), mean firing rates (G), place field size (H), or spatial information (I) between c-Fos positive (orange) and negative (black) place cells. Box plots show median, 1st and 3rd quantiles, and minimum/maximum values within 1.5 x the interquantile range (IQR) from each quantile.
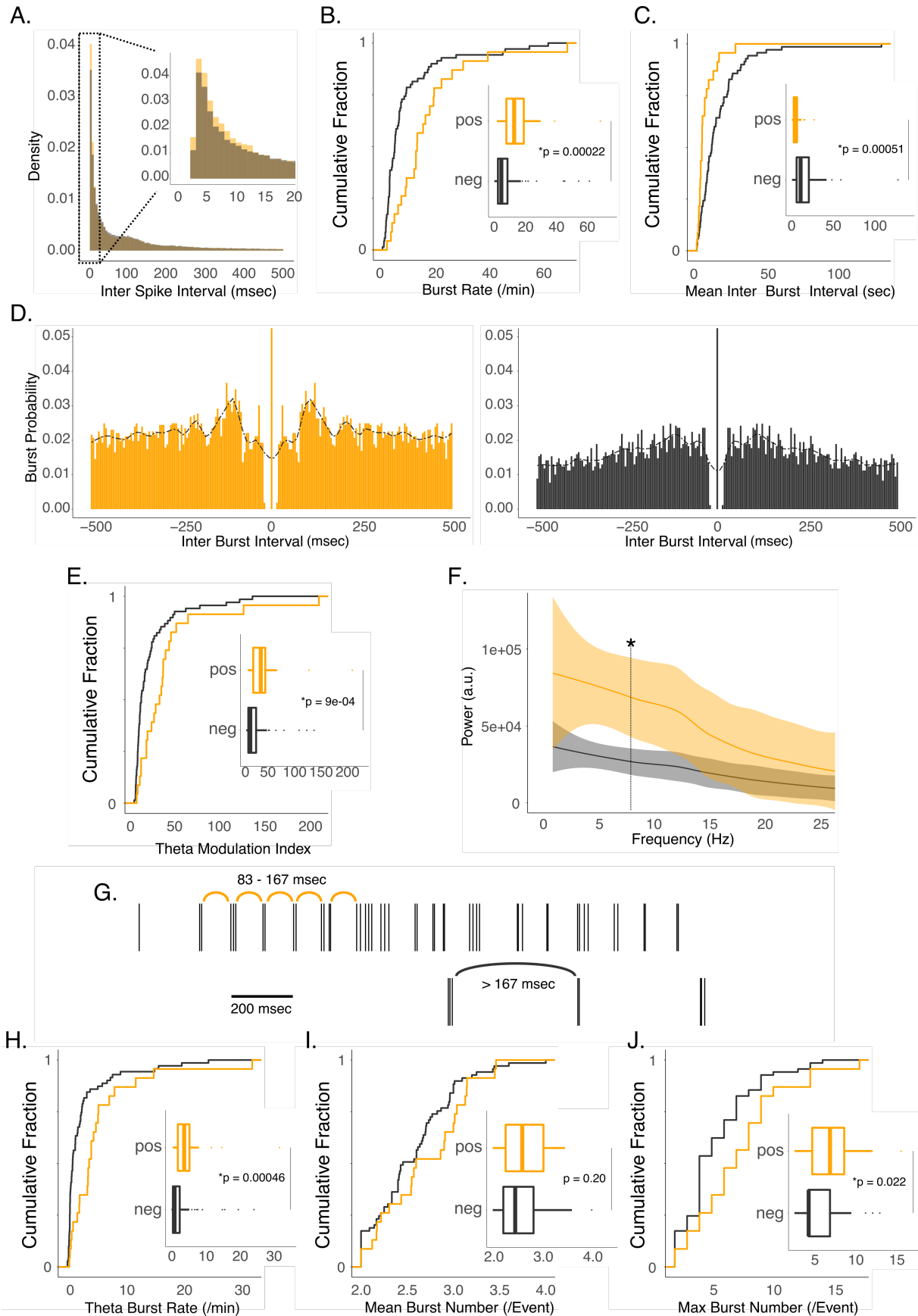
Fig. 2. Theta-paced burst activity in the c-Fos positive place cells. **A.** Histograms showing densities of inter spike intervals from all c-Fos positive (orange) or negative (black) place cells. **B – C**. Cumulative density plots and boxplots comparing burst rates (B) and mean inter burst intervals (C) of the two cell types. **D.** Autocorrelogram of burst activity from an example positive (orange) and negative (black) place cells. Local polynomial regression lines are plotted over the histograms. **E.** Theta modulation index of burst autocorrelograms. **F.** Power spectrograms of burst trains. **G.** Example raster plots showing theta-paced burst events (TBEs; IBI = 83~167 msec) and repetitive bursts outside of the criteria (IBI < 83 msec or IBI > 167 msec). **H – J.** Cumulative density plots and boxplots comparing TBE rates (H), mean burst number per TBE (I), and maximum burst number within a single TBE (J) of the two cell types. Box plots show median, 1st and 3rd quantiles, and minimum/maximum values within 1.5 x IQR from each quantile.
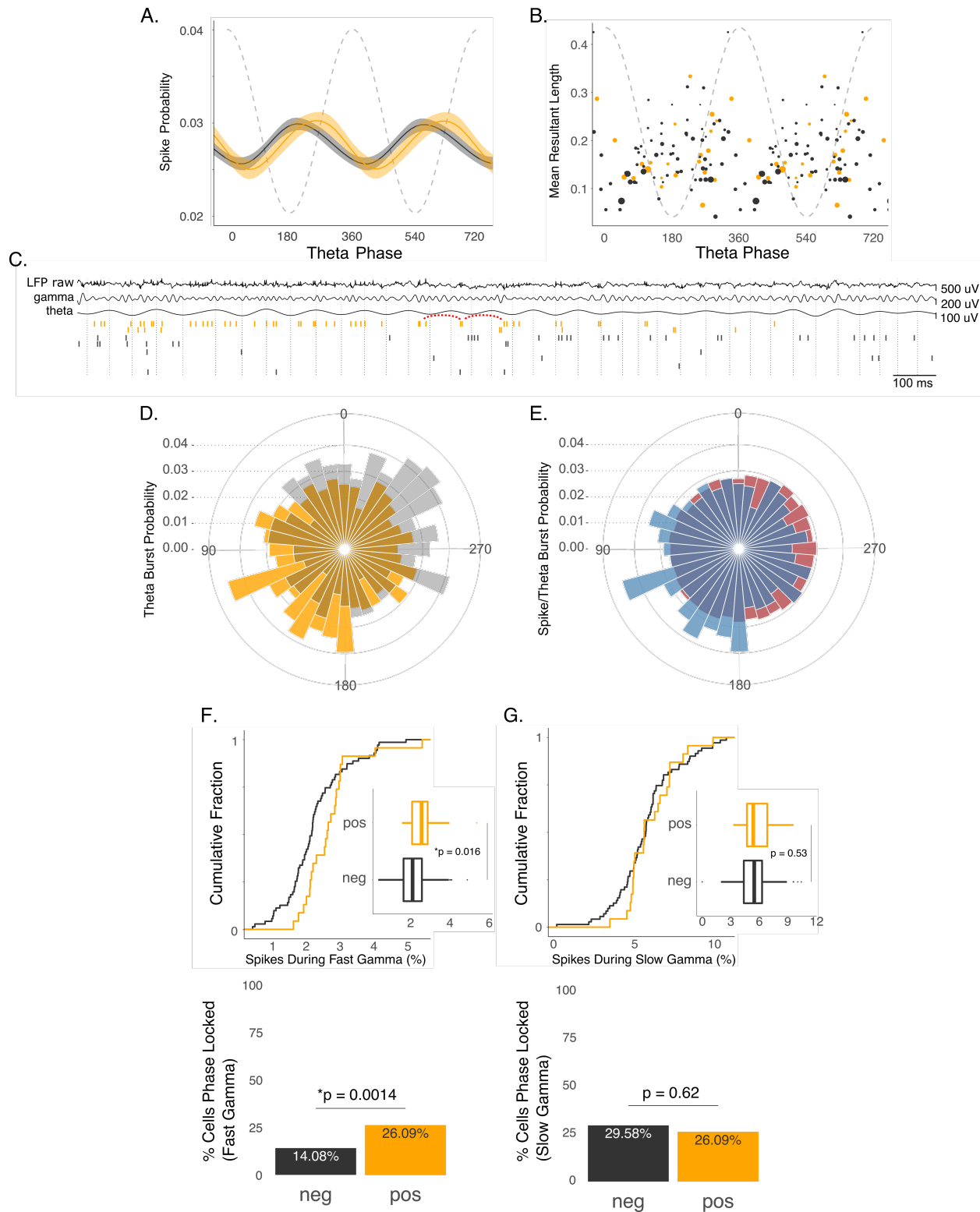
Fig. 3. LFP modulation of spikes from c-Fos positive and negative place cells. **A.** Spike probability of the two types of cells over phases of theta oscillation (6-12 Hz) (pos = orange, neg = black, only significantly phase locked cells are used). Shadows represent confidence intervals. **B.** Mean resultant length of c-Fos positive (orange) or negative (black) cells plotted as s function

of preferred theta phas. Dot size represents mean firing rate of that cell. Only significantly phase locked cells are plotted (pos: 22 cells, neg: 68 cells). **C.** Example spike raster plots with LFP traces (raw, theta filtered (6-12 Hz), gamma filtered (30-85 Hz)). Red arcs represent a TBE occurring at the descending phase of theta. **D.** A roseplot showing TBE spike probability across theta phases (pos = orange, neg = black, 10 degree bins). **E.** A roseplot showing spike probability of c-Fos positive place cells over theta phases (TBE spikes = blue, all spikes = red). **F.** Percent of spikes occurring during fast gamma events (top) and percent cells phase locked to fast gamma (bottom; pos = orange, neg = black). **G.** Percent spikes occurring during slow gamma events (top) and percent cells phase locked to slow gamma (bottom; pos = orange, neg = black). **H.** Percent TBEs occurring during fast (top) or slow (bottom) gamma events. Box plots show median, 1st and 3rd quantiles, and minimum/maximum values within 1.5 x IQR from each quantile.
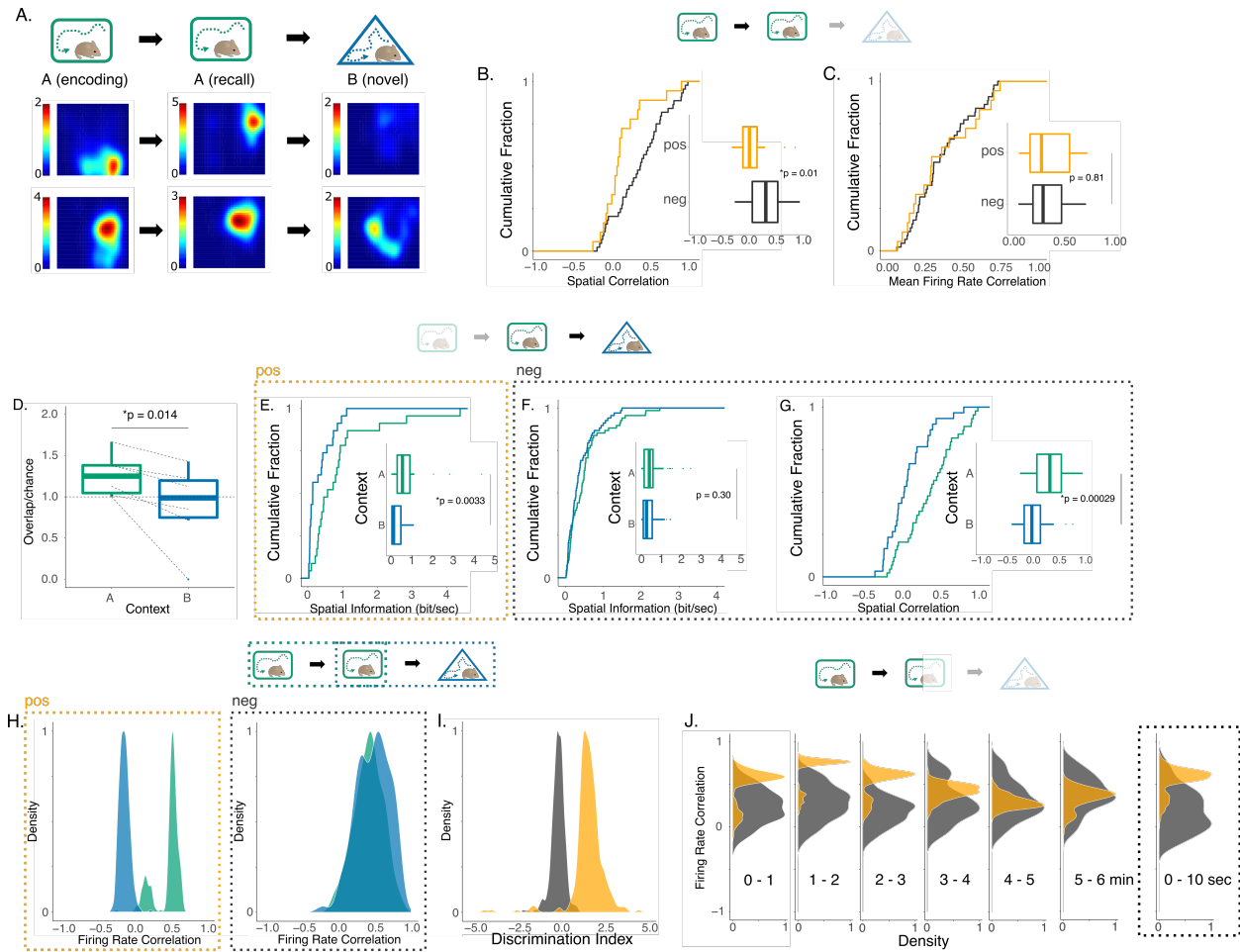
Fig. 4. Different responses of c-Fos positive and negative place cells to the encoding context and a distinct novel context. **A.** Firing rate maps of c-Fos positive (top) or negative (bottom) place cell activity during encoding (left), re-exposure to the encoding context (middle), or exploration of a distinct novel context (right). **B.** Spatial correlation between place maps in A (encoding) and A (recall) (pos = orange, neg = black). **C.** Mean firing rate correlation between place maps in A (encoding) and A (recall) (pos = orange, neg = black). **D.** An animal-by-animal boxplot showing observed overlaps between c-Fos positive cells and place cells normalized by those expected by chances, comparing context A (encoding, green) vs B (novel, blue) sessions. **E – F.** Spatial information of c-Fos positive or negative place cells when animals explore context A (encoding; green) or B (novel; blue). **G.** Spatial correlations between two c-Fos negative place maps in A (encoding; green) and B (novel; blue). **H.** Distribution of ensemble firing rate correlations (see Methods) of c-Fos positive or negative place cells between context A (encoding) – A (recall) (green) vs A (encoding) – B (novel) (blue). **I.** Distribution of discrimination indexes obtained by c-Fos positive (orange) or negative (black) ensemble firing rate correlations. **J.** Instantaneous ensemble firing rate correlations of 6 min of the context A (recall) session binned by 1 min (left), or that of the first 10 sec (right). c-Fos positive place cells in orange, negatives in black. For H-J, values are plotted as probability densities (scaled). Box plots show median, 1st and 3rd quantiles, and minimum/maximum values within 1.5 x IQR from each quantile